



Study on effects of tool nose radius on the formation mechanism of edge defects during milling SiC_p/Al composites

Qiulin Niu¹ · Lu Jing¹ · Changping Li¹ · Zhen Yu² · Shujian Li¹ · Pengnan Li¹ · Xinyi Qiu¹ · TaeJo Ko^{1,2} · Wenhui Yue¹

Received: 3 December 2020 / Accepted: 29 March 2021 / Published online: 7 April 2021
© The Author(s), under exclusive licence to Springer-Verlag London Ltd., part of Springer Nature 2021

Abstract

Silicon carbide particulate reinforced aluminum matrix composites (SiC_p/Al) have received considerable attention in many engineering applications. However, the existence of dispersing SiC particles leads to particularly vulnerable edge quality of SiC_p/Al composites in machining. It is very significant to improve the edge defects of SiC_p/Al composites by optimizing the tool geometry. Cutting tool nose radius mainly determines the machining performance. Therefore, the effects of tool nose radius on the chip topography, cutting force, and edge geometry in face and dry milling of 20% SiC_p/Al composites were investigated in the current work. Experiments were conducted with tool nose radius of 0.5, 1, 1.5, and 2 mm. The results showed that the shorter and wider chips were found with the increment in tool nose radius. It was also observed that the cutting force increased with the increment in tool nose radius. Based on the material removal mechanism with different tool nose radius, the feature maps of edge defects in SiC_p/Al composites were established and studied. It was found that the outer and inner edge quality of the materials was improved with the increase of tool nose radius.

Keywords SiC_p/Al composites · Milling · Tool nose radius · Edge defects

1 Introduction

Silicon carbide particulate reinforced aluminum composites (SiC_p/Al) are a type of metal matrix composites having aluminum alloy as the matrix and are reinforced by nano-sized or micron-sized SiC hard particles. They are widely applied in aerospace, armory, automotive, nuclear, marine, and medical engineering due to their excellent physical and mechanical properties, such as high specific stiffness, high specific strength, small thermal expansion, satisfactory corrosion resisting properties, and so on [1, 2]. Especially, SiC_p/Al composites are often used for processing into thin-walled parts such as structural substrates for space mirrors and electric packaging [3].

Milling is an effective method to obtain SiC_p/Al composites with diverse shapes and large machining allowance, due to which milling is one of the most common processing methods of the materials [4]. However, SiC_p/Al composites always possess the typical low-ductility, inhomogeneity, and anisotropy on account of their particular structure, which lead to poor machinability and even hinder their widespread industrial applications in practice [5, 6]. In this kind of composites, the stress distribution around SiC particles is nonuniform, which causes some phenomena to happen easily like edge breakout, avalanche angle, and burrs [7]. The existence of these edge defects on the workpiece may lead to several problems, for instance, decreasing the convenience of fitting and assembly of parts, damaging the dimensional accuracy and surface finish, increasing the production cost and time due to deburring, endangering the safety of workers, contributing to electrical short circuits, reducing cutting performance and tool life [8–10]. The edge defects have a serious impact on the processing quality and availability of the high-end precision parts, because of which the edge quality problem is especially necessary to be improved.

Therefore, Gaitonde et al. [11] conducted in-depth research in this field and indicated that edge finishing on precision components was more complex. Cao [12] studied the factors

✉ Qiulin Niu
qlniu2009@163.com

TaeJo Ko
tjko@yu.ac.kr

¹ School of Mechanical Engineering, Hunan University of Science and Technology, Xiangtan 411201 Hunan China

² School of Mechanical Engineering, Yeungnam University, Gyeongsan-si Gyeongsangbuk-do South Korea

related to the exit edge defects in milling ceramics using a two-dimensional finite element model. It was concluded that the machined defects could be formed at three regions, which existed at the entrance when the tool initially contacts the workpiece, along the tool path, and when the tool leaves the workpiece, respectively. Chern [8] investigated the influence of cutting conditions on the machined edge in end milling of aluminum alloys, then pointed out that the formation of edge breakout and burrs were strongly dependent upon the in-plane exit angle. Niu et al. [13] conducted milling experiments in SiC_p/Al composites under different cutting parameters; the results showed that the better exit edge shape could be obtained by selecting low or high milling speed, small feed rate, and medium axial cutting depth. Zhou et al. [14] observed that the fracture mechanism of SiC particles had an important influence on the machined surface quality and edge quality of the materials.

Optimizing the tool geometry is an important method to improve the machinability of this kind of difficult-to-cut materials [15–18]. Tool geometry can be approached from many diverse parameters; one of them that mainly determines the processing results is the tool nose radius, which is a very important part of the cutting edge [19, 20]. It is necessary to consider the effects of tool nose because the effective cutting edge is mainly concentrated onto the circular tool nose when the axial cutting depth and tool nose radius are on the same size level [21]. In the milling process, the tool nose radius, rake, and clearance faces are directly in contact with the workpiece. Hence, careful selection of the abovementioned parameters is of prime importance for getting better-machined quality. Bhardwaj et al. [22] found that the surface roughness decreased with the increase in tool nose radius during the milling of AISI 1019 material. On the basis, Kuram [23] performed experiments of milling AISI 304 stainless steel and observed that cutting forces dropped with the increment in nose radius, and the edge serration change trend of chip morphology was related to the change of tool nose radius. Ali Abbasi and Feng [24] evaluated the effects of PCD end mill's nose radius on machinability of titanium alloy Ti-6Al-4V then discovered optimum nose radius for the PCD tool by studying its influence on heat distribution and forces employing finite element simulations. Orra and Choudhury [25] established a mechanistic model based on three-dimensional cutting operations for predicting cutting forces in machining. The model considered the effects of tool nose radius on chip formation and worn-out cutting tool.

As per the literature survey, very limited research work is carried out on the effects of tool nose radius on the milling characteristics of SiC_p/Al composites with hard and brittle property. Furthermore, most researchers limit their studies to relating surface roughness [26], surface micro-morphology

[27], and surface formation mechanism [28] of SiC_p/Al composites, while there are few studies on the edge machined quality and edge formation mechanism. Therefore, an attempt was made to explore the effects of tool nose radius on edge machined quality in milling SiC_p/Al composites. In this research, the influence of tool nose radius on chip morphology, cutting force, and edge geometry of milling 20% SiC_p/Al composites were comprehensively discussed. The mechanism of edge defects and chip formation was analyzed particularly. This work could provide theoretical guidance to assist in selecting the proper tool nose radius to inhibit the edge defects formation of hard and brittle materials.

2 Experimental designs

2.1 Workpiece material

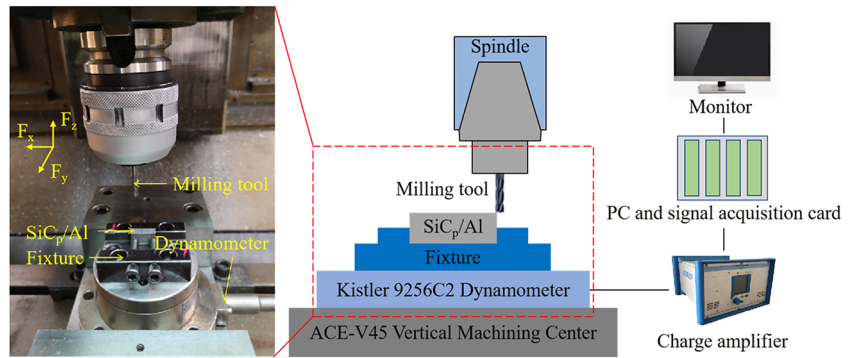
The face milling experiments were conducted on SiC_p/Al composites, in which the volume fraction is 20% and the average size is about 15 μm for SiC particles. The aluminum alloy matrix material belongs to Al-Zn-Mg-Cu series ultra-high-strength aluminum alloy. The size of experimental samples was prepared in the form of 8 mm × 20 mm × 10 mm by cutting in a wire electrical discharge machine. The tools utilized in the experiments were produced by OSG company as HSR 2060 050, HSR 2060 100, HSR 2060 150, and HSR 2060 200 with nose radius 0.5 mm, 1 mm, 1.5 mm, and 2 mm, respectively. They were double-edged solid carbide-coated tools with 30° helix angle and 6 mm diameter, coating TiAlSiN.

2.2 Experiment setup and conditions

All the milling tests were performed on a high-precision vertical machining center ACE-V45 in dry environment. The cutting conditions were cutting speed = 40 m/min; feed per tooth = 0.04 mm/z; axial cutting depth = 0.5 mm; radial cutting depth = 3 mm; tool nose radius = 0.5, 1, 1.5, and 2 mm. During experiments, only tool nose radius was varied while others were held constant to observe the effects of variation of nose radius on the processing results. The experimental setup is schematically illustrated in Fig. 1. Figure 2 shows the schematic diagram of the cutting process between tool nose radius and workpiece in this study.

After testing, the Kistler 9256C2 piezoelectric three-way dynamometer was used to record the cutting force. The fracture geometry of edge defects and chip morphology were viewed by a scanning electron microscope, whose type was S4200.

Fig. 1 Experimental setup for machining trials and schematic diagram



3 Results and discussion

3.1 Chip morphology

Figure 3 shows the morphology of chips with different tool nose radius. The brittleness of SiC_p/Al composites is enhanced by the small cutting depth and the uneven distribution of SiC particles. Thus, the chips are fragment under different tool nose radius. When the tool nose radius is 0.5 mm, the chip edge is irregularly serrated, which is owing to the micro-cracks convergence and propagation caused by SiC particles interferes with the uniform formation of serrated chips. With the increase of tool nose radius, the chips become shorter and wider. As can be seen from Fig. 3, the chip width increases by 62.53% when the tool nose radius increases from 0.5 to 2 mm. Besides, the edge cracks decrease, which is related to the increase of cutting heat derived from extrusion friction between the tool and the workpiece improves the plastic deformation of the cutting layer.

Figure 4 is the schematic of chip formation. During chip formation, the micro-cracks initiate on the free surface and extend to the chip root near the tool nose. The thickness of chip root decreases with the increase of tool nose radius. The

pressure exerted on the workpiece by the tool nose cutting edge causes the chip tearing and shortening. Additionally, the wider chips are visible due to the contact length between the cutting edge and the cutting layer increases with the increase of tool nose radius.

3.2 Cutting force

In the analysis of cutting force, which can be resolved into three components: the feed force (F_x), the tangential force (F_y), and the axial force (F_z). The variation of cutting force with tool nose radius can be seen in Fig. 5. It is observed that the cutting force shows an increasing trend as the tool nose radius increases continually. When the tool nose radius is 2 mm, F_z is 3 times that when the tool nose radius is 0.5 mm. This is attributed to the fact that there is a higher stress gradient at the arc cutting edge when the tool nose radius is small, which causes larger shear stress. However, the material removal mechanism changes gradually with the increase of tool nose radius. As can be seen from Fig. 6, the cutting-edge angle κ_r decreases with the increment in tool nose radius, which results in the shape of the instantaneous

Fig. 2 Schematic diagram of cutting process between tool nose radius and workpiece

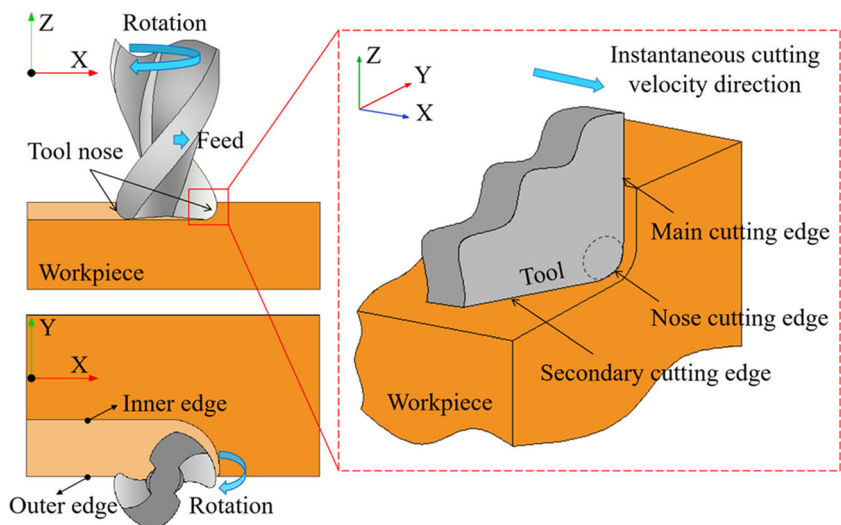
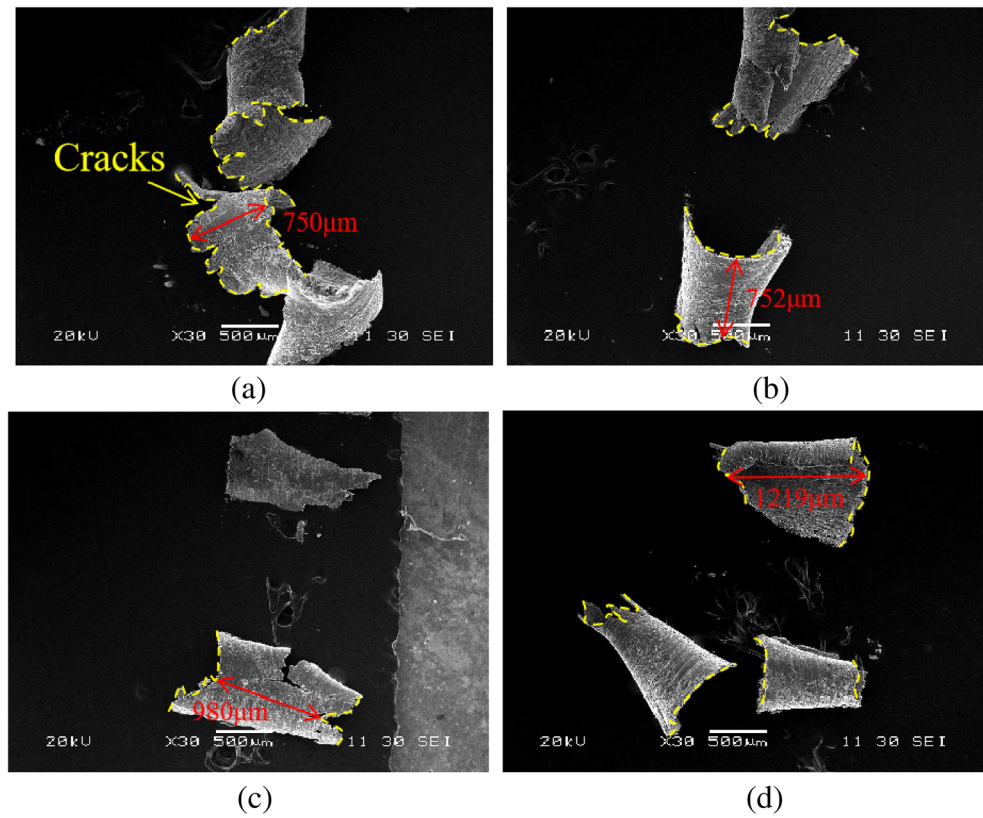


Fig. 3 The changes of the morphology of chips with tool nose radius: **a** $R=0.5$ mm, **b** $R=1$ mm, **c** $R=1.5$ mm, **d** $R=2$ mm



cutting zone formed by the tool nose arc cutting edge becoming narrower and longer. Then, the material at the tool nose is transformed from the shear failure to the accumulation extrusion failure, increasing the ploughing effect between the arc cutting edge and the workpiece. The improvement of ploughing effect leads to more serious material deformation, higher specific cutting energy, and larger cutting force. In addition, the increasing length of the cutting edge who contacts with

the workpiece makes the possibility of interaction between the cutting edge and SiC particles enhanced. Namely, the force required for SiC particles to be pulled out, pressed in and broken increases when tool nose radius increases while other conditions remain unchanged.

Figure 5 also illustrates that the axial force F_z is relatively large when tool nose radius reaches 0.5 mm. This may be due to the fact that the distribution of SiC particles in the workpiece is nonuniform in the axial direction when tool nose

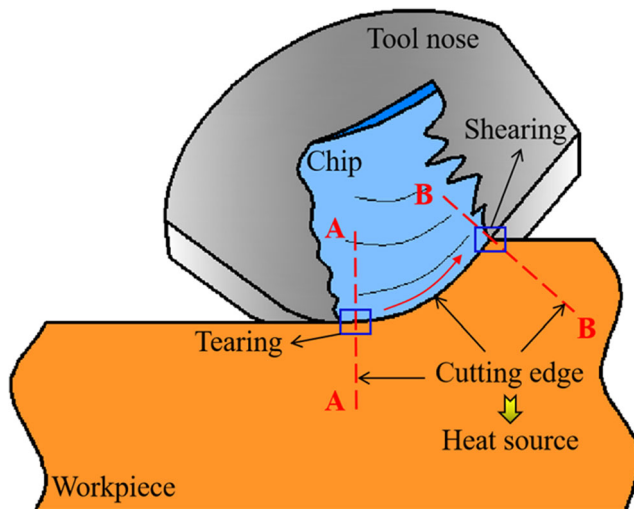


Fig. 4 Schematic of chip formation

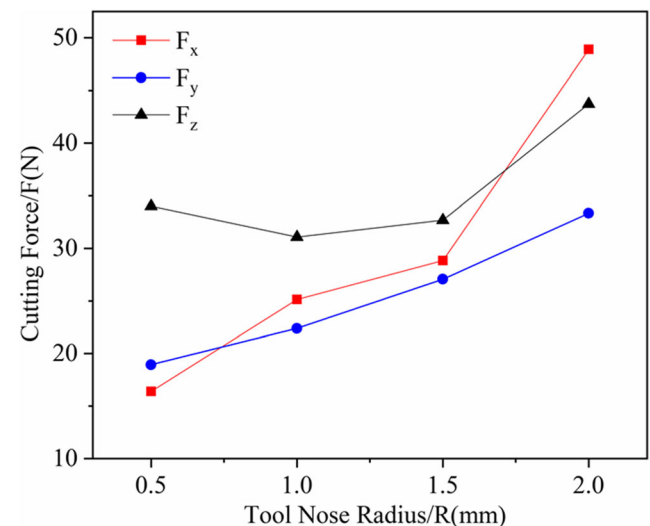
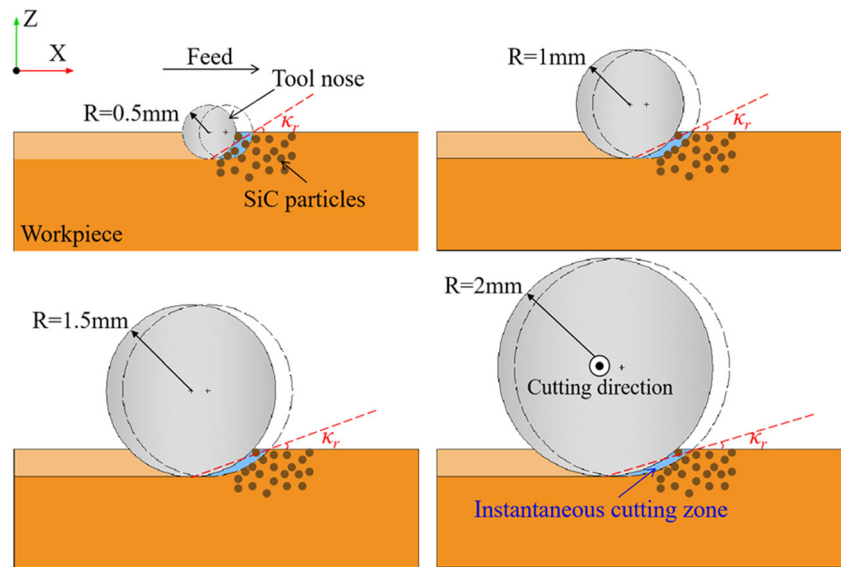


Fig. 5 The variation of cutting force with tool nose radius

Fig. 6 Schematic model of instantaneous cutting zone of tool nose radius



radius is 0.5 mm, which leads to more SiC particles in contact with the tool and larger cutting force is produced. This phenomenon does not affect the overall variation trend of cutting force.

3.3 Outer edge geometry

According to the machining characteristics of this study, the generation of outer edge defects in one feed cycle can be divided into three stages:

- I. The tool nose cutting edge is just in contact with the workpiece, which is the extrusion friction stage between the tool cutting edge and the workpiece. This stage is characterized by the initiation of cracks and chips in the workpiece.
- II. Continuous milling stage, in which cutting extrusion is carried out.
- III. The tool teeth withdraw from the workpiece, and the tool nose gradually extends to the outer edge of the workpiece, forming a negative shear angle. This results in the edge material sliding in the shear direction, then forming edge defects eventually. In the third stage, the elastic-plastic deformation zone at the tool nose has a different deformation mechanism with the different tool nose radius. The tool nose radius affects the formation mechanism of edge defects directly.

The material deformation schematic at the cutting edge of tool nose is shown in Fig. 7. The material at the tool nose cutting edge deforms under the double action of extrusion and shearing, and the machining results are discrepant with the difference in their proportion. When the tool nose radius is small, the cutting deformation of SiC_p/Al composites is

dominated by the shear deformation. Under this condition, the outer edge is short of supporting force, and the plastic deformation extends to the area below the cutting layer, which is easy to generate large edge spalling. The impact of cutting edge on SiC particles is mainly crushing and pulling out. With the further increase of tool nose radius, the negative shear angle at the cutting edge tends to decrease, which improves the influence of the compressive stress on the edge material. Namely, the ploughing effect of the cutting edge on SiC_p/Al composites increases. The strength of the workpiece under compressive stress is greater than that under shear stress and tensile stress, together with the SiC particles can strengthen the aluminum matrix, which leads to a small amount of edge collapse. At the same time, few broken SiC particles are found due to their tiny elastic effect.

With the increase of tool nose radius, the changes of the outer edge geometry are given in Fig. 8. When the tool nose radius is 0.5 mm, there is a serious aluminum matrix spalling phenomenon on the machined outer edge. In addition, the tearing aluminum matrix is accompanied by the shedding, fracture, and breakage of SiC particles. When the tool nose radius is 1 mm, the plastic flow of the aluminum matrix containing broken SiC particles occurs, coupled with the presence of friction between the tool and the workpiece. Those factors result in material bonding on the outer edge. At this point, the outer edge is seriously damaged. However, when the tool nose radius reaches 1.5 mm, a small amount of edge spalling and aluminum ductile fracture appear. The outer edge quality is the best when the tool nose radius is 2 mm, where only slight spalling occurs.

In addition, it can be seen from Fig. 8 that when the tool nose radius changes from 0.5 to 2 mm, the surface damages near the outer edge caused by SiC particles, such as pits, particle breakage, micro-cracks, and other defects, change to

be dominated by aluminum matrix coating gradually. This phenomenon can be explained that the SiC particles are easy to be cut off due to the increase of cutting force, and the increase of cutting heat can improve the ductility of SiC_p/Al composites. Therefore, when the tool nose radius increases, the tool nose pushes the aluminum matrix to fill the cavity and make up for the cracks on the surface. The plastic flow of aluminum is beneficial to improve the quality of the machined surface and edge.

3.4 Inner edge geometry

The formation of the machined outer edge is mainly due to the cutting extrusion at the bottom of the tool nose arc cutting edge, while the machined inner edge is formed by the contact area between the tool nose and the inner edge. The change of tool nose radius has a significant influence on the stress state of the inner edge and the formation mechanism of its defects.

Figure 9 provides the SEM images of the inner edge geometry. When the tool nose radius is 0.5 mm and 1 mm, a large area of the plastic bulge can be seen on the inner edge of the workpiece. However, the defects on the inner edge change into particles spalling in concentrate and aluminum matrix spalling gradually with the increase of tool nose radius.

When the tool nose radius reaches 2 mm, only tiny aluminum matrix spalling occurs. It can be observed that the quality of the machined inner edge is improved with the increase of tool nose radius.

The formation mechanism of inner edge defects is illustrated in Fig. 10. The formation of inner edge defects is mainly affected by two directions: “direction A” is the pushing and extruding direction of the tool nose cutting edge; “direction B” is the direction of downward pressure to the material by tool nose cutting edge. It can be seen from the stress state of the inner edge that with the increase of tool nose radius, the inner edge material will be subjected to higher compressive stress N and smaller push stress f . Therefore, the inner edge material is pushed more when the tool nose radius is small, resulting in the plastic flow of the aluminum matrix along “direction A,” forming plastic bulge. When the tool nose radius is large, the inner edge material is mainly subjected to compressive stress. Meanwhile, the joint between SiC particles and the aluminum matrix is easy to cause dislocation accumulation, which will induce stress concentration. In this state, the interface between SiC particles and aluminum matrix is easy to debond under the extrusion friction of the tool nose. It results in cracks and drives the aluminum matrix to produce a concentrated spalling phenomenon in “direction B.” Because of the fact that SiC_p/Al

Fig. 7 Material deformation schematic at the cutting edge of tool nose

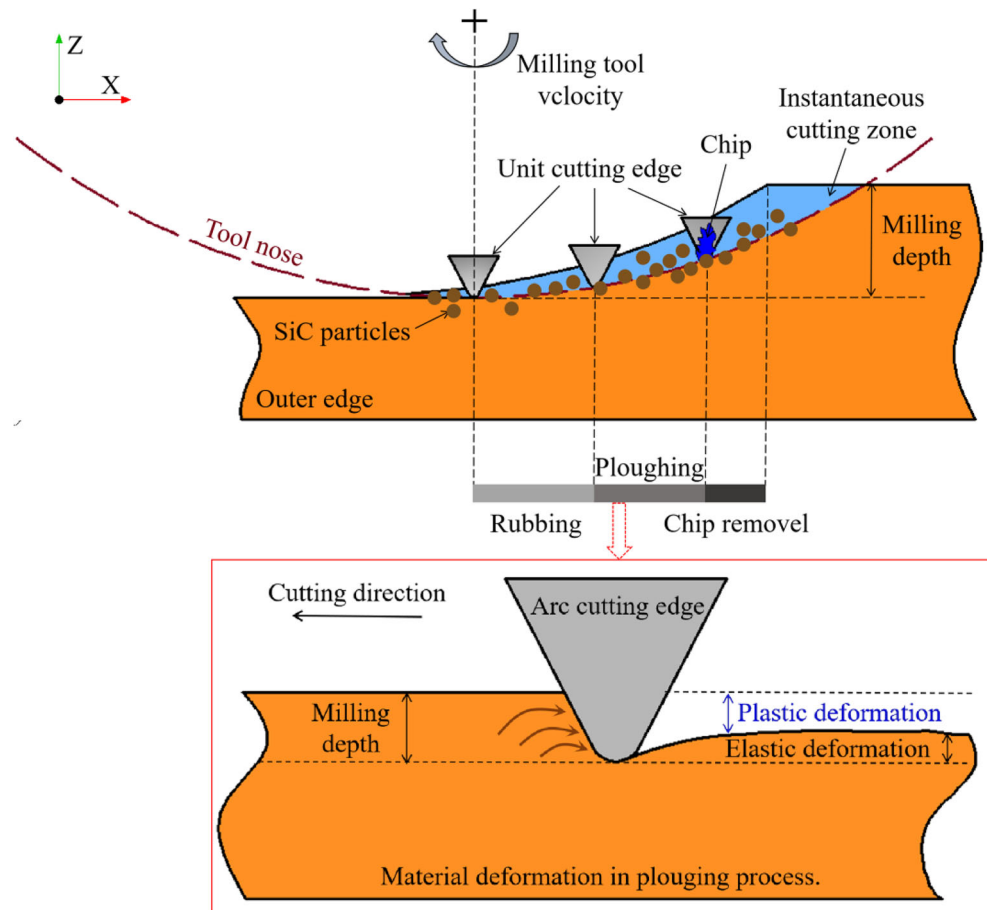


Fig. 8 The changes of the outer edge geometry with tool nose radius: **a** $R=0.5$ mm, **b** $R=1$ mm, **c** $R=1.5$ mm, **d** $R=2$ mm

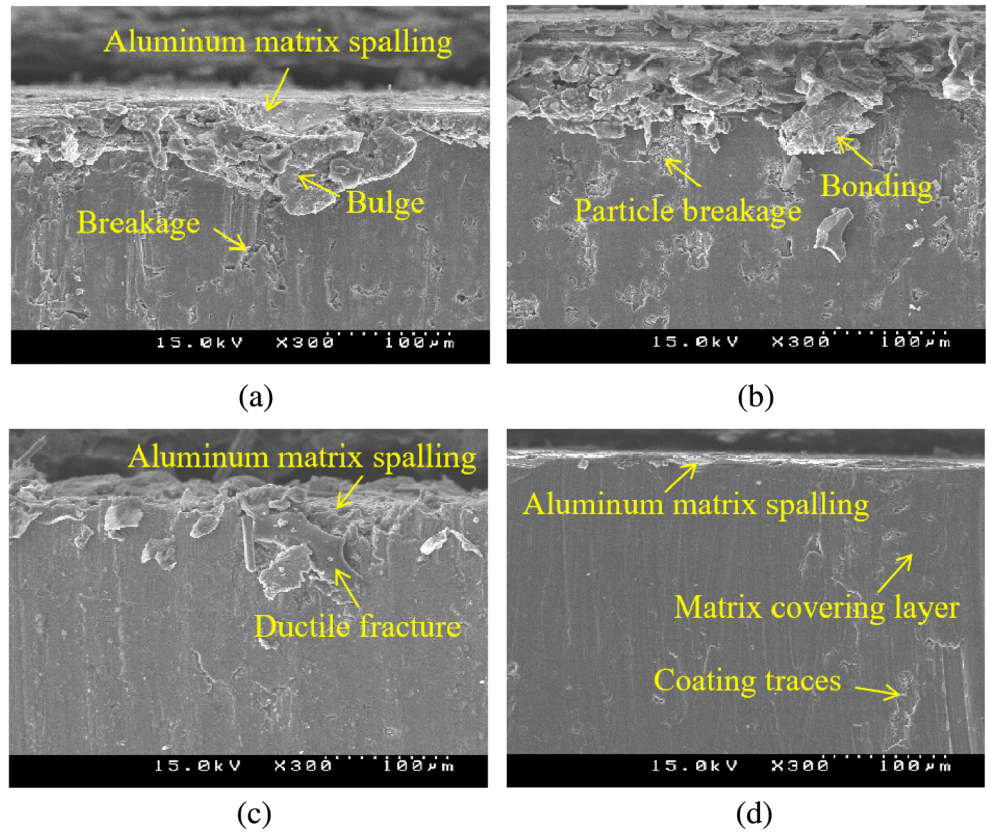


Fig. 9 The changes of the inner edge geometry with tool nose radius: **a** $R=0.5$ mm, **b** $R=1$ mm, **c** $R=1.5$ mm, **d** $R=2$ mm

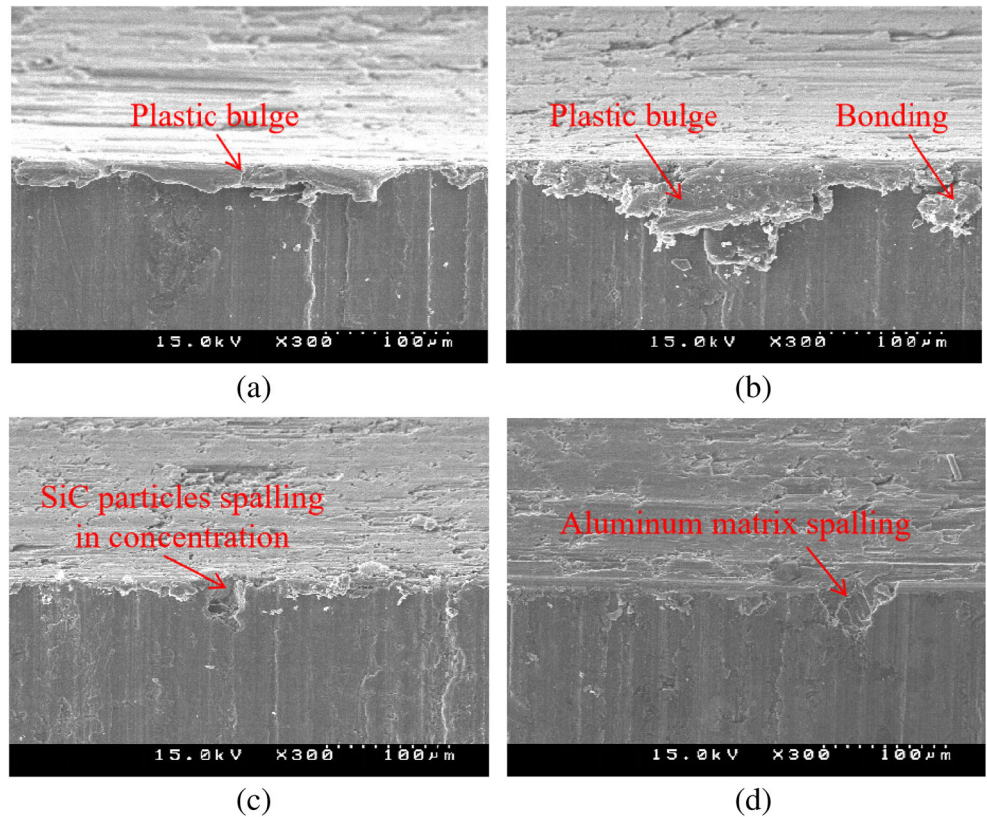
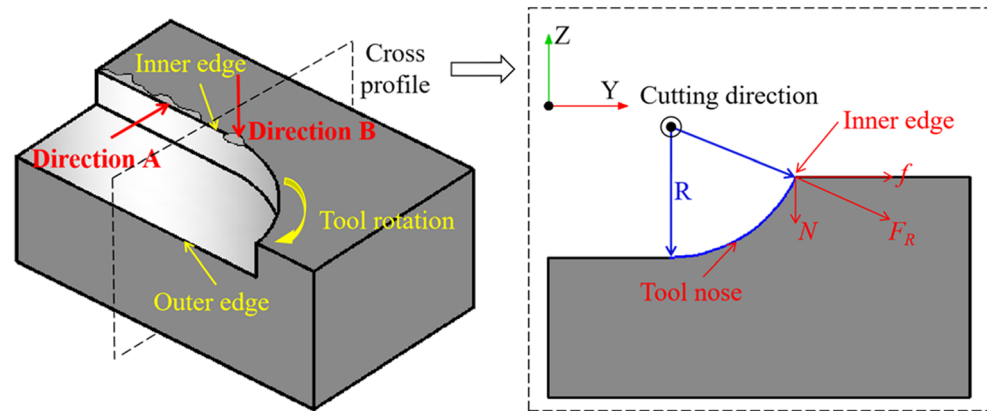


Fig. 10 Formation mechanism of inner edge defects



composites are more stable under compressive stress, it can be concluded that the quality of the inner edge is improved with the increase of tool nose radius.

4 Conclusions

In the current study, the effects of tool nose radius on chip morphology, cutting force, and edge geometry were discussed during the milling of 20% SiC_p/Al composites. The achieved results were summarized as follows:

1. It is observed that the chips become shorter and wider, coupled with chip edge cracks decrease with the increment in tool nose radius. The chip width increases by 62.53% when the tool nose radius increases from 0.5 to 2 mm.
2. With the increase of tool nose radius, the ploughing effect between the arc cutting edge and the workpiece increases, resulting in all force components (F_x , F_y , F_z) increase. When the tool nose radius is 2 mm, F_z is 3 times that when the tool nose radius is 0.5 mm.
3. When the tool nose radius changes from 0.5 to 2 mm, the machined outer edge defects such as edge spalling and failure change into slight spalling and ductile fracture. The formation of inner edge defects is affected by two directions: the pushing and extruding direction, and the direction of downward pressure. The direction of impact on the inner edge varies with the tool nose radius. When the nose radius reaches 2 mm, only tiny defects occur. With the increase of tool nose radius, the quality of the outer and inner edges is improved.
4. When the cutting depth is less than the tool nose radius, the machinability of SiC_p/Al composites is improved with the increase of tool nose radius, which is regard to the double action of extrusion and shearing. Especially, this research is of great help to study the influence of tool nose radius on workpiece edge geometry. Then, it is able to explore the processing quality of SiC_p/Al composites with different cutting parameters or tool structures in future work.

Author contribution Qiulin Niu, Changping Li, and TaeJo Ko conceived the central idea of the study; Lu Jing, Zhen Yu, and Xinyi Qiu analyzed the data; Qiulin Niu and Lu Jing interpreted the results; Lu Jing wrote the initial draft of the paper; Shujian Li, Pengnan Li, and Wenhui Yue contributed to refining the ideas and carried out additional analyses. All authors discussed the results and revised the manuscript.

Funding This work is funded by the National Natural Science Foundation of China (no. 52075168, 51605161, 51975208), the Project of Department of Education of Hunan Province (no. 19B190), and the Scientific Research Fund of Hunan University of Science and Technology (no. KJ-2042).

Availability of data and material The data and material in this paper are original, available, and objective.

Code availability Not applicable.

Declarations

Ethical approval Not applicable.

Consent to participate Not applicable.

Consent for publication We would like to submit the manuscript entitled “Study on effects of tool nose radius on the formation mechanism of edge defects during milling SiC_p/Al composites” by Qiulin Niu, Lu Jing, Changping Li, Zhen Yu, Shujian Li, Pengnan Li, Xinyi Qiu, TaeJo Ko, and Wenhui Yue, and we wish to be considered for publication in the International Journal of Advanced Manufacturing Technology.

Competing Interests The authors declare no competing interests.

References

1. Huang ST, Guo L, Yang HC, Su Y, Xu LF (2019) Study on characteristics in high-speed milling SiC_p/Al composites with small particles and high volume fraction by adopting PCD cutters with different grain sizes. *Int J Adv Manuf Technol* 102(9):3563–3571
2. Sun W, Duan CZ, Yin WD (2020) Development of a dynamic constitutive model with particle damage and thermal softening for SiC_p/Al composites. *Compos Struct* 236:111856
3. Wang T, Wu XY, Zhang GQ, Dai YQ, Xu B, Ruan SC (2020) An experimental study on single-point diamond turning of a 55 vol%

- SiC_p/Al composite below the ductile brittle transition depth of SiC. *Int J Adv Manuf Technol*
4. Niu QL, Jing L, Wang CH, Li SJ, Qiu XY, Li CP, Xiang DH (2020) Study on effect of vibration amplitude on cutting performance of SiC_p/Al composites during ultrasonic vibration-assisted milling. *Int J Adv Manuf Technol* 106(2):2219–2225
 5. An QL, Chen J, Ming WW, Chen M (2020) Machining of SiC ceramic matrix composites: A review. *Chinese J Aeron*
 6. Zhu CM, Gu P, Liu DH, Hu X, Wu YY (2019) Evaluation of surface topography of SiC_p/Al composite in grinding. *Int J Adv Manuf Technol* 102:2807–2821
 7. Jiao KR, Huang ST, Xu LF, Zhou DJ (2015) Feature classification of high-volume SiC_p/Al composites under the condition of two-dimensional cutting based on cluster analysis theory. *Int J Adv Manuf Technol* 78:677–686
 8. Chem GL (2006) Experimental observation and analysis of burr formation mechanisms in end milling of aluminum alloys. *Int J Mach Tool Manu* 46(12-13):1517–1525
 9. Dong GJ, Lang CY, Li C, Zhang LM (2020) Formation mechanism and modelling of exit edge-chipping during. *Ceram Int* 46(8):12458–12469
 10. An QL, Dang JQ, Li JL, Wang CY, Chen M (2020) Investigation on the cutting responses of CFRP/Ti stacks: with special emphasis on the effects of drilling sequences. *Compos Struct* 253:112794
 11. Gaitonde VN, Kamik SR, Achyutha BT, Siddeswarappa B (2006) Taguchi approach with multiple performance characteristics for burr size minimization in drilling. *J Sci Ind Res* 65(12):977–981
 12. Cao YQ (2001) Failure analysis of exit edges in ceramic machining using finite element analysis. *Eng Fail Anal* 8(4):325–338
 13. Niu QL, Tang LY, Liu X, Li PN, Qiu XY (2017) Influence of cutting parameters on edge morphology of SiC_p/Al matrix composites in milling. *Aerosp Mater Technol* 47(5):35–39 in Chinese
 14. Zhou L, Wang Y, Ma ZY, Yu XL (2014) Finite element and experimental studies of the formation mechanism of edge defects during machining of SiC_p/Al composites. *Int J Mach Tool Manu* 84:9–16
 15. Najjar KA, Sheikh NA, Butt MM, Shah MA (2018) Enhancing the wear resistance of WC-Co cutting inserts using synthetic diamond coatings. *Ind Lubr Tribol* 70(7):1224–1233
 16. Dong GJ, Zhang LM (2019) Investigation on grinding force and machining quality during rotary ultrasonic grinding deep-small hole of fluorophlogopite ceramics. *Int J Adv Manuf Technol* 104(5-8):2815–2825
 17. Jin K, Wei B, Roy A, Jones LCR, Ayvar-Soberanis S, Silberschmidt VV (2019) Hybrid machining of metal-matrix composite. *Procedia CIRP* 82:184–189
 18. Deng B, Peng FY, Zhou L, Wang HW, Yang MH, Yan R (2020) A comprehensive study on flank wear progression of polycrystalline diamond micro-tool during micro end-milling of SiC_p/Al composites. *Wear* 456-457:203291
 19. Dong GJ, Wang L, Li C, Yu YF (2020) Investigation on ultrasonic elliptical vibration boring of deep holes with large depth-diameter ratio for high-strength steel 18Cr2Ni4WA. *Int J Adv Manuf Technol* 108(5-6):1527–1539
 20. Brown I, Schoop J (2020) The effect of cutting edge geometry, nose radius and feed on surface integrity in finish turning of Ti-6Al4V. *Procedia CIRP* 87:142–147
 21. Wang T, Xie LJ, Wang XB (2015) Simulation study on defect formation mechanism of the machined surface in milling of high volume fraction SiC_p/Al composite. *Int J Adv Manuf Technol* 79(5-8):1185–1194
 22. Bhardwaj B, Kumar R, Singh PK (2014) Effect of machining parameters on surface roughness in end milling of AISI 1019 steel. *P I Mech Eng B-J Eng* 228:704–714
 23. Kuram E (2016) Nose radius and cutting speed effects during milling of AISI 304 material. *Mater Manuf Process* 32(2):185–192
 24. Ali Abbasi S, Feng PF (2015) Evaluating the effect of PCD end mill's nose radius on machinability of titanium alloy Ti-6Al-4V in high speed milling. *Appl Mech Mater* 713-715:217–222
 25. Orra K, Choudhury SK (2018) Mechanistic modelling for predicting cutting forces in machining considering effect of tool nose radius on chip formation and tool wear land. *Int J Mech Sci* 142–143:255–268
 26. Liu JW, Cheng K, Hui, et al. (2016) An investigation of surface defect formation in micro milling the 45% SiC_p/Al composite. *Procedia CIRP* 45:211–214
 27. Du J, Zhang H, He W, Ma J, Ming W, Cao Y (2019) Simulation and experimental study on surface formation mechanism in machining of SiC_p/Al composites. *Appl Compos Mater* 26(1):29–40
 28. Zhang PF, Zhou L, Ran YC (2019) Finite element analysis and comparison of the machinability of SiC_p/Al composite and CNT/Al composite. *J Inst Eng India Ser C* 101(8)

Publisher's note Springer Nature remains neutral with regard to jurisdictional claims in published maps and institutional affiliations.